RSC Advances

ROYAL SOCIETY OF CHEMISTRY

www.rsc.org/advances

Insight into crystallization process of rubrene by binary solvent mixtures

Lijuan Wang [a*], Yiping Li[b], Fengjun Zou[a], Hao Du[b], Lijing Sun[a], Jidong Zhang[c], Xiaofeng Song[a], Guicai Song[b]

[a]School of Chemical Engineering, Changchun University of Technology, Changchun 130012, PR China

[b]School of Science, Changchun University of Science and Technology, Changchun 130022, PR China

[c]State Key Lab of Polymer Physics and Chemistry, Changchun Institute of Applied Chemistry, Chinese Academy of Science, Changchun 130022, PR China

Abstract

Solution-processing rubrene crystals were fabricated by blending an amount of high-boiling-point solvent into the rubrene dilute solution in chloroform. The crystallization processes were investigated by the analysis of morphology and crystalline structures. The trajectory to the pathways during dendrite-like crystals growth was clearly observed by controlling the ratio of the binary solvent mixtures. The tremendous, compact dendrite-like crystals and the sheet-like crystals were obtained by further reducing the evaporation rate by drop-casting method. The results indicated that the crystalline process was significantly influenced by the binary solvent ratio and the fabrication methods. The crystalline of rubrene films could be tuned from disorder, with pure chloroform solvent, to high crystalline, with binary solvent mixtures. The formation mechanism of rubrene crystals was proposed as competition between the impetus of slow evaporation by high-boiling-point solvent and the self-assembly force of rubrene molecules to the

* Corresponding author. Tel.: +86 431 85712368
E-mail address: wlj15@163.com (L. Wang).

crystal. These results, which exhibit the concrete possibility of growing crystalline and ordered rubrene thin films, open perspectives to organic thin film technology and devices.

Keywords: solution-processing, crystal growth, rubrene, binary solvents

1. Introduction

Organic semiconductor crystals have received wide attention with the rapid development of organic electronic. Rubrene (5,6,11,12-tetraphenylnaphthacene), which possesses the long exciton diffusion length [1] and high charge carrier mobility of 20 cm^2/Vs,[2] has been recognized as one of the most representative and promising organic material in actual devices.[3-5] Rubrene single-crystal transistors have been produced by weak epitaxy growth method in vacuum.[6] And the high quality crystalline rubrene films have been obtained by organic molecular beam epitaxy.[7] However, it is crucial for us to explore an easy method for obtaining rubrene film with desired crystalline morphology. During the past several years, solution-processable methods such as spin-coating or drop-casting, which belong to very simple and inexpensive approaches, have been proposed for preparing organic crystals.[8] And the performance of polymer devices has obtained significant progress by the control of the morphology and structure by using solution-processable methods.[9,10] The slow growth of solution processes has enhanced crystalline domains and self-organization of polymer films by using a high-boiling-point solvent.[11,12] The small molecule organic films by solution-processable methods also show the significant progresses, such as high-boiling-point solvents,[13,14] double solvent approach,[15] and appropriate amounts of additives.[16] However, the solution growth of rubrene crystals with high mobility properties lies in the initial stages of investigation in blending an amount of polymer into rubrene solution [17] and using various organic solvents [18]. It is still challenging to achieve the good processing characteristics and high crystalline order of small-molecular species with high mobility. In this work, the issues regarding the crystallization of rubrene in binary solvent mixtures were investigated. The binary solvent system comprised a weak polar solvent and a strong polar solvent, for example, mixtures of

chloroform plus N,N-dimethylformamide (DMF) with different chloroform/DMF ratios (v/v). Based upon the drying behavior, the morphology of rubrene crystals was manipulated by making use of the relative evaporation rate of the two solvents.

2. Experiment section

2.1 Materials

Rubrene with purity greater than 99% was purchased from Sigma-Aldrich (USA). Chloroform ($CHCl_3$, 99 %) and N,N-dimethylformamide (DMF, 99 %) were purchased from Beijing Chemical Works (China). All materials and solvents were used as received without further purification. The chemical structure of rubrene used in this work was shown in Fig. 1a.

2.2 Substrate preparation

A heavily doped n-type silicon wafer with a 300 nm thermal oxidation SiO_2 layer was used as the substrate. The substrates were carefully cleaned in a piranha solution (70:30 v/v of concentrated H_2SO_4 and 30% H_2O_2) at 90 °C for 20 min. Then the substrates were thoroughly rinsed in sequence of acetone, alcohol and deionized water. Finally, the substrates were dried by the stream of nitrogen and heated at 70 °C for 10 min to remove solvent traces.

2.3 Film preparation

The dilute solution was obtained by first dissolving rubrene (2 mg) in chloroform of 0.5 ml. Then, the DMF solvent of high boiling point was very slowly added to the dilute solution, as shown in Fig. 1b. The volumes of adding DMF solvents were 0.1 ml, 0.3 ml, and 0.4 ml, whose mixed ratios of chloroform to DMF were 0.5:0.1, 0.5:0.3, and 0.5:0.4 (v:v), respectively. Before use all the solutions were placed at room temperature overnight for the complete dissolution of the solutes. All the experiments were performed at room temperature (RT) of 22 °C.

To prepare the semiconductor layer, both spin-coating and drop-casting were carried out in ambient conditions, as shown in Fig. 1c and d. In the spin-coating process, the rubrene solutions with different solvent ratios were cast for 30 s at a rate of 2250 rpm. In the drop-casting process, 50 μl DMF solvent and 50 μl dilute solution of rubrene in chloroform of 0.5 ml were continuously deposited on the SiO_2/Si substrates with a size of 1.5 cm × 1.5 cm. The mixed ratios of chloroform to DMF corresponded to 0.5:0.5 (v:v). In this work, the conditions of solution used as precursors were shown in Table 1. And the deposition methods, the boiling point, the captions of the images and some results were simultaneously included in Table 1.

2.4 Characterization

Polarized optical microscopy (POM) was taken with a polarized optical microscope (Leica DMRX, Germany) in reflection mode through two crossed polarizer. Atomic force microscopy (AFM) images were obtained by using a SPA-300HV instrument with a SPI3800N Controller (Seiko Instruments Inc., Japan) in tapping mode. A silicon microcantilevel (spring constant 15 Nm^{-1} and resonant frequency 130 kHz, Nanosensors, Switzerland) was used for the scanning. The scanning electron microscopy (SEM) images were obtained by using FEI XL 30. The X-ray diffraction (XRD) pattern was taken from a D8 Discover thin-film diffractometer (Bruker, Germany) with Cu Kα radiation (λ = 1.54056 Å). The selected voltage and current were 40 kV and 35 mA, respectively. The X-ray profile was recorded from 2° to 30° in steps of 0.05° by using automatic slits.

3. Results and discussion

In the following part, firstly, rubrene crystals obtained by the mixture of chloroform/DMF binary solvent will be demonstrated. After that, the morphology and crystalline structures of rubrene

crystals will be depicted. At last, the possible mechanism for the formation of rubrene crystals will be proposed.

3.1 The fabrication of rubrene crystals based on binary solvent

The films of rubrene were first prepared through the spin-coating method, in which pure chloroform and binary solvent mixtures were used as solvent, respectively. The optical microscope and SEM images of the crystalline films were shown in Fig. 2. It was clear that the morphology of rubrene films with pure chloroform solvent and with binary solvent mixtures of adding 0.1 ml DMF significantly differed. In Fig. 2a and a_1, the rubrene film could not be observed from the optical microscope images. By using SEM in Fig. $2a_2$, some dispersed remnants of rubrene were clearly observed. It was relatively difficult to obtain rubrene films dissolved in pure chloroform solvent without DMF due to the poor film-forming property of the molecule. In Fig. 2b and b_1, the dendrite-like morphology was observed based on binary solvent of 0.5:0.1 (v/v) chloroform/DMF. In a sample size of 3 × 3 mm, there was no preferential orientation of the dendrite-like gains (optionally). And some self-aggregations of rubrene molecules around the dendrite-like domains were observed, as shown in Fig. $2b_2$. It exhibited the coexistence of dendrite-like crystals and self-aggregations of rubrene molecules with binary solvent mixtures of adding 0.1 ml DMF. It thus concludes that the binary solvent mixture has a much more remarkable promoting effect on the crystallization of rubrene than the pure chloroform solvent. The similar dendrite-like morphology has been observed in triisopropylsilyl (TIPS) pentacene films spin-coated from solvents which have high boiling points.[13]

3.2 The influence of the binary solvent ratios on the formation of rubrene crystals

The growth procedure of the dendrite-like crystals was further investigated by using SEM. It was

noted that rubrene crystal morphologies encompassed information about the crystal growth processes. A binary solvent mixture by adding different DMF volumes in the solution of 2 mg rubrene per 0.5 ml chloroform solvent was spin-coated on the SiO_2/Si substrates. The dendrite-like crystals were all obtained, as shown in Fig. 3.

In Fig. 3a, the trajectory to the pathways during dendrite-like crystals growth was clearly observed by chloroform/DMF of 0.5/0.1 (v/v) or the final concentration of 3.33 mg/ml. The three morphologies, which confirmed the migration of rubrene molecules, were in concurrence due to the 0.1 ml DMF solvent addition to rubrene mixture. Firstly, the self-aggregation of rubrene molecules was observed, as shown in Fig. $3a_1$. Then the self-assembly rubrene molecules were extended and ribbon-like crystals were obtained in the process of the migration along the crystal nuclei, as shown in Fig. $3a_2$. Ribbon-like crystals continued to migrate in connection with certain part of dendrite-like crystals. Finally, uniform lamellar structures were obtained, as shown in Fig. $3a_3$. The formation of dendrite-like crystals was attributed to the increase of migration ability for rubrene molecules towards the existing crystal nuclei with increasing the DMF volumes. N,N-dimethylformamide (DMF), having higher boiling points (153 °C [19]), could reduce the evaporation rate of solvent and provide mobility for rubrene molecules to migrate to the crystal nuclei. In this work, experimental boiling points of solvent were shown in Table 1. The pure chloroform solvent was 61 °C, which was accordant to the literature [13,17]. The boiling points of binary solvent increased with the increasing volume of DMF, which was 78 °C in chloroform/DMF of 0.5/0.1 (v:v) and was 97 °C in chloroform/DMF of 0.5/0.4 (v:v). But the boiling points lay in between 61 °C of pure chloroform solvent and 153 °C of pure DMF solvent. As a result, coexistence of dendrite-like crystals and rubrene molecules was observed in

chloroform/DMF of 0.5/0.1 (v:v). The partial rubrene molecules could not migrate to the crystal nuclei due to the low DMF addition volumes and insufficient migration ability.

In Fig. 3b, the formation of denser dendrite-like crystals was observed due to the sufficient migration ability of rubrene molecules towards the exiting crystal nuclei. In Fig. 3c, however, sparse and small dendrite-like crystals were obtained by the binary solvent mixtures of chloroform/DMF of 0.5/0.4 (v/v) or the final concentration of 2.22 mg/ml. It was attributed to the reduction of an amount of crystal nuclei per ml. And few rubrene molecules could move to the crystal. In large magnification, distinctive lamellar structures with various thicknesses could be clearly observed in dendrite-like crystals, as shown in Fig. $3b_1$ and c_1. The formation of lamella as primitive forms of crystals was detected by the clear presence of the crystal growth front. But the self-aggregation of rubrene molecules and ribbon-like crystals could not be observed, which was attributed to the sufficient migration ability of rubrene molecules in DMF solvent addition of 0.3 ml and 0.4 ml. Consequently, the growth velocity of the rubrene dendrite-like crystals depended significantly on the adding amount of DMF solvent. The migration force supplied to the rubrene molecules by the solvent molecules has been proved in solvent vapor.[17] The formation of supramolecular aggregation for 5,6,11,12- tetrachlorotetracene was obtained by the addition of polar hydroxyl groups from methanol.[15]

3.3 The influence of the film fabrication on the formation of rubrene crystals

The spin-coating procedure has a faster evaporation rate of solvent than the drop-casting one. To further investigate the crystallization of rubrene, the films were prepared through the drop-casting method with slow evaporation rate. Drop-casting was carried out in oven of 80 °C, 60 °C, and in an ambient clean room environment, respectively. The morphologies of the crystalline films were

shown in Fig.4. As can be seen, the rubrene molecules assembled into the dendrite-like crystals in oven of 80 ℃ and 60 ℃ temperatures, which was similar to the crystalline morphology of spin-coating. However, in drop-casting process, the shape and size of the dendrite-like crystals became more tremendous and compact than those in spin-coating process, as shown in Fig. 4a and b. The corresponding SEM and AFM images of the films were shown in Fig. $4a_1$,a_2 and b_1,b_2. Distinctive lamellar structures were obtained, which dominated in the films. As can be seen, the rubrene molecules were assembled into lamellar structures. Rubrene crystals with lamellar structures were connected with certain part of dendrite-like crystals. However, in an ambient room environment, the crystalline morphologies changed significantly in Fig. 4c. Sheet-like crystals were obtained and the shape of dendrite-like crystals could hardly be seen in POM images. By using SEM and AFM analysis, it was clearly observed that the sheet-like crystals were still made up of dendrite-like crystals in Fig. $4c_1$ and c_2. Compact branching was aligned in the sheet-like crystals and the spaces of the branching were reduced. The formation of rubrene crystals was accordant to that by spin-coating process. The results indicated that the growth procedure of rubrene crystals was controlled by the evaporation rate of solvent and the binary solvent provided the sufficient mobility for rubrene molecules to migrate to the crystal nuclei.

3.4 The crystalline structure of rubrene crystals

XRD was performed to investigate the crystalline structures of rubrene films deposited by solution. The X-ray diffraction patterns of the drop-cast films by binary solvent and pure solvent were shown in Fig. 5. For the initial rubrene films with pure chloroform solvent, no well defined diffraction was recorded (Fig. 5I). On rubrene films with the binary solvent mixtures of chloroform/DMF, intense diffraction peaks indicative of crystalline order developed, as shown in

Fig. 5 II, III. Single crystal rubrene had an orthorhombic structure with unit cell parameters a=14.44 Å, b=7.18 Å , c=26.97 Å, and the space group was Aba2.[20] In Figure 5II, the most strong and sharp diffractive peak at 2theta = 6.75°, corresponding to an inter-planar distance of 13.09 Å, was observed. We could attribute the peak to the (002) diffraction of the rubrene single crystal. The data were in accordance with the orthorhombic structure reported for rubrene.[20,21] A weak diffractive peak at 2theta = 20.39°, corresponding to an inter-planar distance of 4.35 Å, could also be seen. It could be attributed to the (006) diffraction of the rubrene crystal, which were the third of the (002) peak. The results indicated that the diffraction peaks were assigned to the orthorhombic structure. In the crystalline film, the rubrene molecules arranged mainly with the *c* axis perpendicular to the substrate. It was also worth mentioning that an additional weak diffractive peak at 2theta = 12.3°, corresponding to an inter-planar distance of 7.19 Å, was present. It corresponded to the (200) diffraction of rubrene crystal, which indicated that some of the molecules oriented with *a* axis perpendicular to the substrate. And the (400) diffraction of the rubrene crystal was observed, which was the secondary of the (200) peak. The coexistence of both (002) and (200) diffractions demonstrated that the rubrene molecules were arranged with two types of orientation in the normal direction of the substrate. The phenomenon could be attributed to the fast evaporation of the binary solvent in oven of 80 °C.

In Figure 5III, the diffractive peaks of (002) and (200) could also be obtained at room temperature in ambient clean environment. This was similar to the situation in Figure 5II. However, it was noted that the other diffraction peaks were also observed. The series of diffraction peaks were calculated by the above set of crystal unit parameters, which coincided with the observed data very well, as shown in Table 2. Hence, the crystal unit cell parameters were

reasonable. The increased diffraction intensity and better definition of a few specific diffraction peaks for III in comparison with II were due to "texture formation", as was confirmed in the literature.[21] The appearance of the more additional peak was induced by the incomplete orientation of rubrene molecules in the perpendicular direction. The results confirmed that improved molecular ordering and device performance were related to film formation rate. Slower solvent evaporation and film formation rate, which were encouraged by high-boiling-point solvent and drop casting, facilitated the growth of highly ordered films.

3.5 The mechanism of the formation of rubrene crystals

Based on binary solvent approach [15,16,22] and form of spherulites [17,23], a schematic representation of the dendrite-like crystal and sheet-like crystal was proposed to depict the growth process of rubrene crystals, as shown in Fig. 6. The initial nuclei of rubrene molecules were random in the orientation and formed the self-aggregation of initial nuclei by the aggregation. The spiky ribbon-like crystals were formed in the migration process of rubrene molecules. Crystallization was initiated by inserting a slight branch without orientation preference. The results attributed to the impetus of slow evaporation by high-boiling-point solvent. The branching gradually maintained a space filling characteristic due to the self-assembly force of rubrene molecules to the crystal. Ultimately, the sheet-like crystals were formed with reducing the space of the branching. Thus, the aggregation acted as nucleation seeds for the crystallization of rubrene thin films, and then organic molecules migrated with the solvent molecules because of evaporation, and assembled themselves into ordered structure. The slow growth processes enhanced crystalline domains and self-organization of rubrene films by using a high-boiling-point solvent. Appropriate amounts of DMF solvent additives were found to induce the formation of well-ordered crystalline

domains. From the morphology and crystallizing kinetics of rubrene crystals, we can see that the crystals belong to anisotropic growth. Polycrystalline morphologies were obtained by repeating the anisotropic growth.

4. Conclusion

In summary, the crystals of small molecule rubrene were obtained by the solution-processable methods and the crystallization process was studied. The transformation from self-aggregation of initial nuclei to the formation of dendrite-like crystals was observed by controlling the ratio of the binary solvent mixtures in spin-coating. The results were attributed to reducing the solvent evaporation rate by adding the DMF solvent with high boiling point and providing the sufficient migration ability for rubrene molecules. The tremendous, compact dendrite-like crystals and the sheet-like crystals were obtained by further reducing the evaporation rate by drop-casting method. And it was confirmed that the dendrite-like crystals were composed of lamellar structures and the sheet-like crystals were still made up of dendrite-like crystals. The increased diffraction intensity indicated that improved molecular ordering and device performance were related to adding the high-boiling-point solvent. The formation mechanism of rubrene crystals was proposed as the competition between the impetus of slow evaporation by high-boiling-point solvent and the self-assembly force of rubrene molecules to the crystal. Thus, the method, which facilitated the growth of highly ordered films, can be beneficial for a wide range of opto-electronic applications and may offer a straightforward process for the realization of organic semiconductor crystals.

Acknowledgements

This work was financially supported by the National Natural Science Foundation of China

(21403016), Key Program for Science and Technology Development of Jilin Province of China (20130102065JC and 20140203018GX), and Scientific Research Foundation of Education Department of Jilin Province of China (2015103).

References

1 H. Najafov, B. Lee, Q. Zhou, L. C. Feldman, and V. Podzorov, *Nat. Mater.,* 2010, **9**, 938-943.

2 J. Takeya, M. Yamagishi, Y. Tominari, R. Hirahara, Y. Nakazawa, T. Nishikawa, T. Kawase, T. Shimoda, and S. Ogawa, *Appl. Phys. Lett.,* 2007, **90**, 102120.

3 V. C. Sundar, J. Zaumseil, V. Podzorov, E. Menard, R. L. Willett, T. Someya, M. E. Gershenson, and J. A. Rogers, *Science,* 2004, **303**, 1644-1646.

4 D. Braga and G. Horowitz, *Adv. Mater.,* 2009, **21**, 1473-1486.

5 A. L. Briseno, S. C. B. Mannsfeld, M. M. Ling, S. H. Liu, R. J. Tseng, C. Reese, M. E. Roberts, Y. Yang, F. Wudl, and Z. N. Bao, *Nature,* 2006, **444**, 913-917.

6 H. Chang, W. Li, H. Tian, Y. Geng, H. Wang, D. Yan, and T. Wang, *Org. Electron.,* 2015, **20**, 43-48.

7 L. Raimondo, E. Fumagalli, M. Moret, M. Campione, A. Borghesi, and A. Sassella, *J. Phys. Chem. C,* 2013, **117**, 13981-13988.

8 F. G. D. Pozo, S. Fabiano, R. Pfattner, S. Georgakopoulos, S. Galindo, X. Liu, S. Braun, M. Fahlman, J. Veciana, C. Rovira, X. Crispin, M. Berggren, and M. Mas-Torrent, *Adv. Funct. Mater.,* 2015 (DOI: 10.1002/adfm.201502274), 1-8.

9 F. J. M. Hoeben, P. Jonkheijm, E. W. Meijer, and A. P. H. J. Schenning, *Chem. Rev.,* 2005, **105**, 1491-1546.

10 M. J. Winokur and W. Chunwachirasiri, *J. Polym. Sci. Part B: Polym. Phys.,* 2003, **41**, 2630-2648.

11 G. Li, Y. Yao, H. Yang, V. Shrotriya, G. Yang, and Y. Yang, *Adv. Funct. Mater,* 2007, **17**, 1636-1644.

12 J.-F. Chang, B. Sun, D. W. Breiby, M. M. Nielsen, T. I. Sölling, M. Giles, I. McCulloch, and H. Sirringhaus, *Chem. Mater.,* 2004, **16**, 4772-4776.

13 Y.-H. Kim, Y. U. Lee, J.-I. Han, S.-M. Han, and M.-K. Han, *J. Electrochem. Soc.,* 2007, **154**,

H995-H998.

14 S. K. Park, T. N. Jackson, J. E. Anthony, and D. A. Mourey, *Appl. Phys. Lett. ,* 2007, **91**, 063514-063513.

15 Z. He, N. Lopez, X. Chi, and D. Li, *Org. Electron.,* 2015, **22**, 191-196.

16 G. J. Chae, S.-H. Jeong, J. H. Baek, B. Walker, C. K. Song, and J. H. Seo, *J. Mater. Chem. C,* 2013, **1**, 4216-4221.

17 Y. Su, J. Liu, L. Zheng, Z. Ding, and Y. Han, *RSC Adv.,* 2012, **2**, 5779-5788.

18 M. Takeshi, T. Yoshinori, T. Tsukasa, S. Kenichi, M. Yusuke, H. Nobuhiro, T. Yukihiro, M. Norihisa, Y. Masashi, A. Masayuki, T. Junichi, K. Yasuo, M. Yusuke, M. Seizo, and S. Takatomo, *Jpn. J. Appl. Phys.,* 2008, **47**, 8950-8954.

19 R. S. Ramadevi, P. Venkatesu, M. V. P. Rao, and M. Ramakrishna, *Thermochim. Acta.,* 1996, **277**, 133-144.

20 D. E. Henn, W. G. Williams, and D. J. Gibbons, *J. Appl. Crystallogr.,* 1971, **4**, 256.

21 N. Stingelin-Stutzmann, E. Smits, H. Wondergem, C. Tanase, P. Blom, P. Smith, and D. d. Leeuw, *Nat. Mater.,* 2005, **4**, 601-606.

22 X. Li, B. K. C. Kjellander, J. E. Anthony, C. W. M. Bastiaansen, D. J. Broer, and G. H. Gelinck, *Adv. Funct. Mater.,* 2009, **19**, 3610-3617.

23 L. Gránásy, T. Pusztai, G. Tegze, J. A. Warren, and J. F. Douglas, *Phys. Rev. E: Stat., Nonlinear, Soft Matter phys.,* 2005, **72**, 011605.

Figure captions

Fig.1. (a) The chemical structure of rubrene molecule. (b) Schematic illustrations of solution preparation with binary solvent. (c) and (d) Schematic illustrations of film preparation by spin-coating and drop-casting, respectively.

Fig.2 The optical microscope images of spin-coated rubrene films from dilute solution with (a) pure chloroform solvent and (b) binary solvent mixtures of adding 0.1 ml DMF. The corresponding optical microscope (a_1, b_1) and SEM images (a_2, b_2) indicating the detailed surface morphologies. (Micrographs taken with unpolarized light).

Fig.3 SEM images of rubrene films from the solution of 2 mg rubrene in 0.5 ml chloroform solvent by adding various DMF volume. The binary solvent mixtures of chloroform/DMF with various volume ratios (a) 0.5/0.1 (v/v); (b) 0.5/0.3 (v/v); (c) 0.5/0.4 (v/v), respectively. The corresponding SEM images indicating the crystal growth were shown in (a_1), (a_2), (a_3), (b_1), and (c_1).

Fig.4 The cross-polarized optical micrographs of rubrene crystals by drop-casting from binary solvent mixtures of chloroform/DMF under different environments. (a) oven of 80 °C, (b) oven of 60 °C, (c) an ambient clean room environment (micrographs taken with polarized light, 90° to the polarizer/analyzer system). The SEM images of corresponding thin film were shown in (a_1), (b_1) and (c_1). And the AFM images of corresponding thin film were shown in (a_2), (b_2) and (c_2) indicating the detailed surface morphologies.

Fig.5 X-ray diffraction patterns of rubrene crystals dispersed on SiO_2/Si substrate with pure chloroform solvent (I) and with binary solvent mixtures of chloroform/DMF (II and III). After deposition, II was in oven of 80 ℃ and III was in ambient clean environment at room temperature of 22 ℃.

Fig.6 Schematic representation of growth of rubrene crystals by the binary solvent.

Table 1 Summary of the fabrication of rubrene crystals in this work, which included the precursor solution condition, deposited methods, boiling point of solvents, corresponding caption of images and some results.

Chloroform/ DMF (v:v)	Deposited methods	Boiling point	Image captions	Some Results
0.5:0	Spin-coating at RT	~ 61 °C	Fig.2 (a)	Dispersed rubrene remnant
0.5:0.1	Spin-coating at RT	~ 78 °C	Fig.2 (b)	Optional dendrite-like domain
0.5:0.1	Spin-coating at RT	~ 78 °C	Fig.3 (a)	Coexistence of crystals and molecules
0.5:0.3	Spin-coating at RT	~ 86 °C	Fig.3 (b)	Denser dendrite-like crystals
0.5:0.4	Spin-coating at RT	~ 97 °C	Fig.3 (c)	Sparse and small dendrite-like crystals
0.5:0.5	drop-casting at 80 °C	~ 110 °C	Fig.4 (a)	Tremendous dendrite-like crystals
0.5:0.5	drop-casting at 60 °C	~ 110 °C	Fig.4 (b)	Compact dendrite-like crystals
0.5:0.5	drop-casting at RT	~ 110 °C	Fig.4 (c)	Sheet-like crystals

Table 2 Details of d spacing values of different lattice planes for rubrene crystal.

2θ(deg)	d_{obs}(Å)	(hkl)	d_{cal}(Å)
6.75	13.09	(002)	13.49
7.65	11.55	(101)	12.73
10.35	8.54	(003)	8.99
12.3	7.19	(200)	7.22
13.77	6.43	(004)	6.74
15.35	5.77	(203)	5.63
19.37	4.58	(302)	4.53
20.39	4.35	(006)	4.50
24.82	3.59	(400)	3.61
27.83	3.20	(404)	3.18

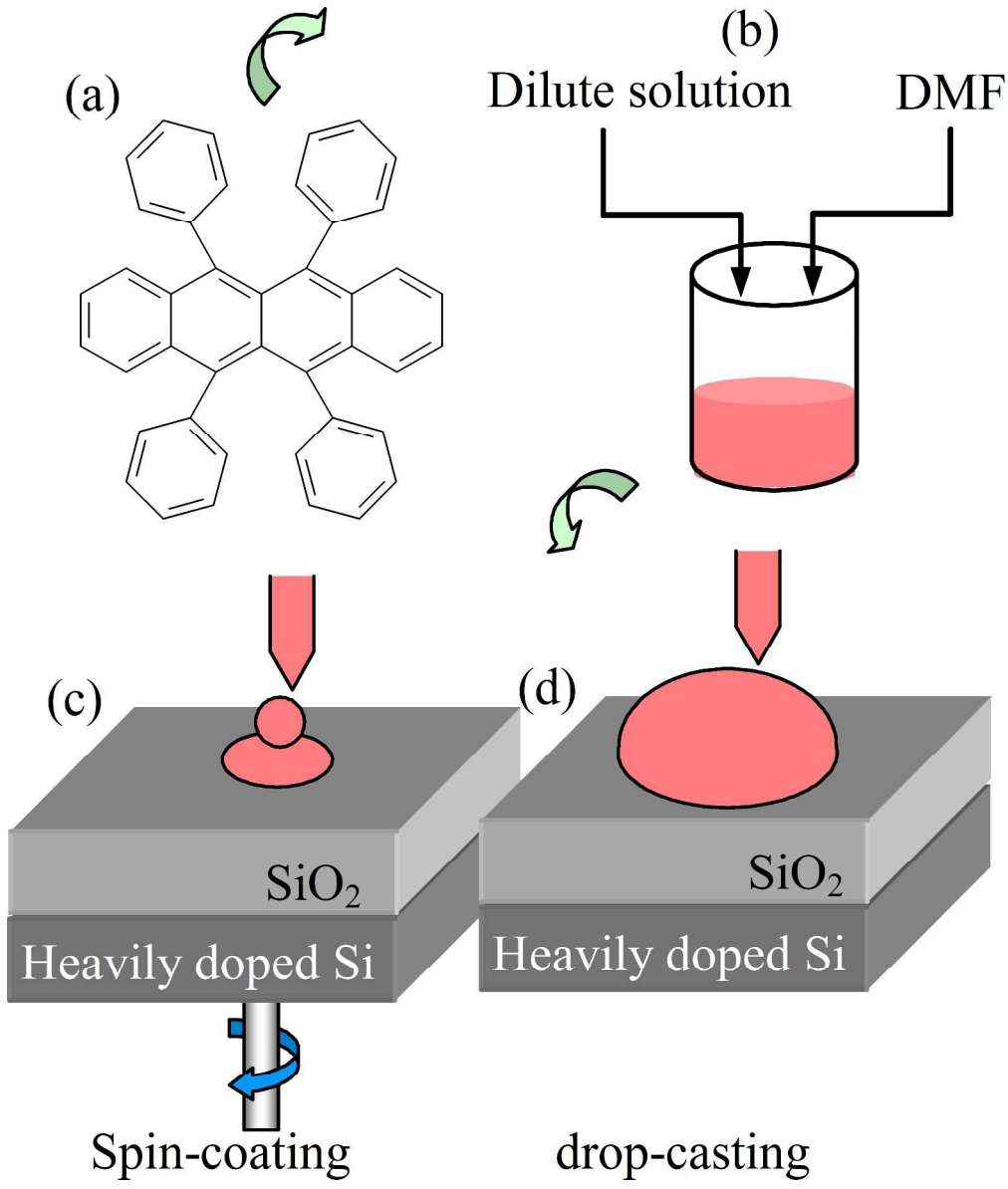

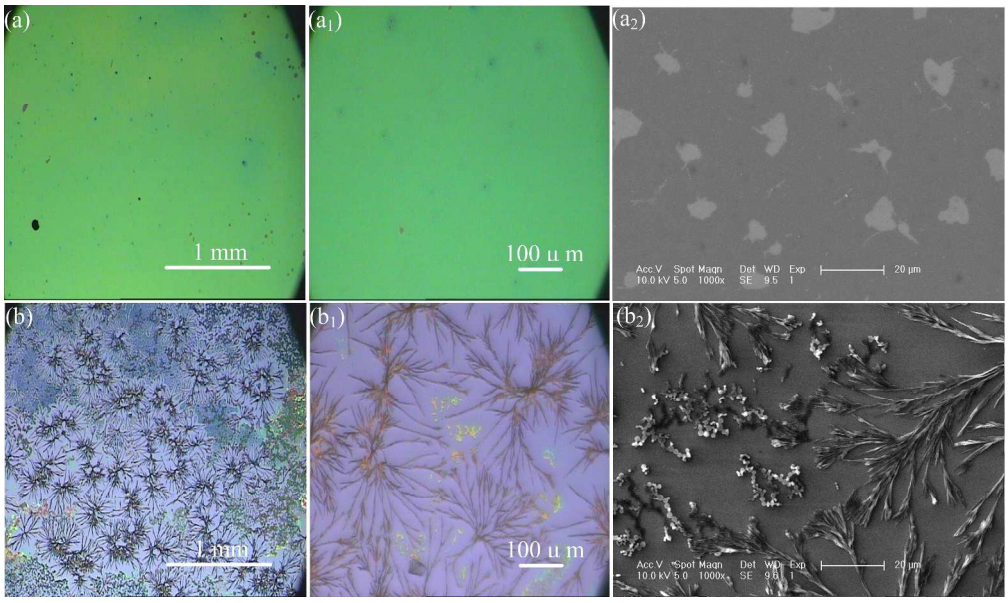

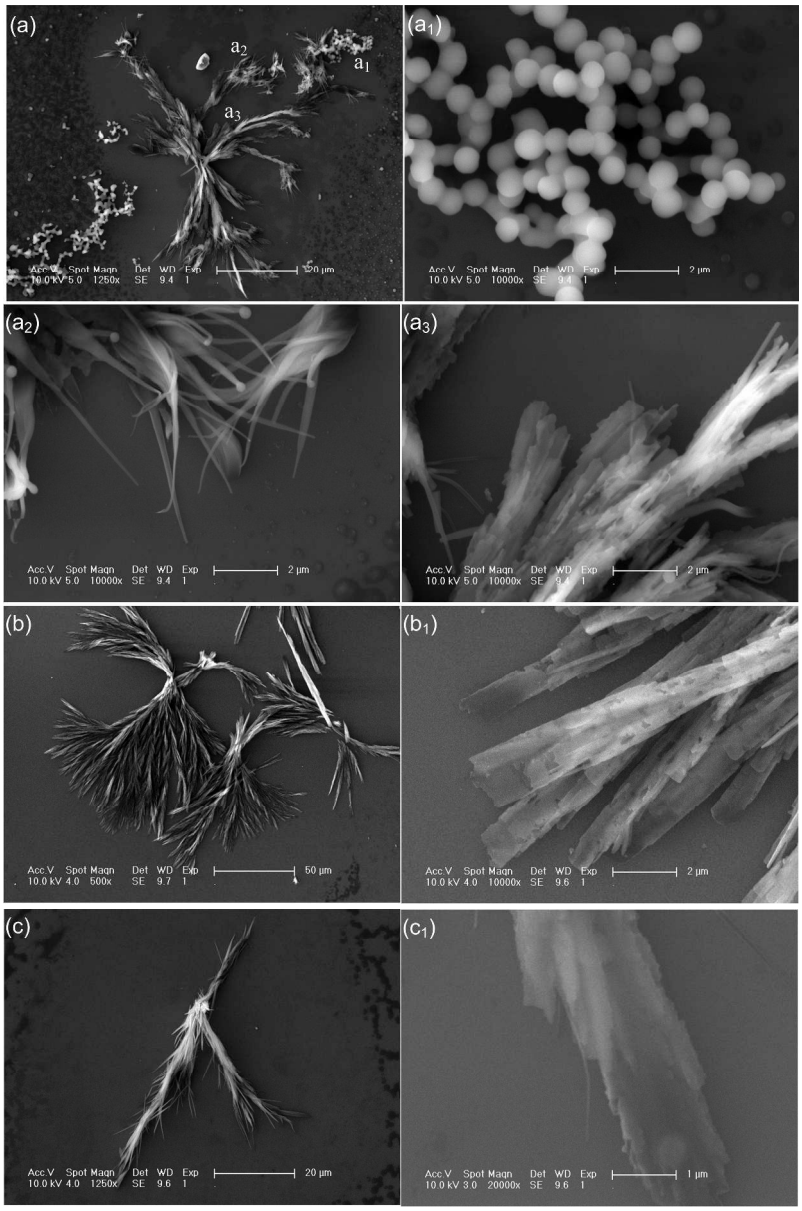

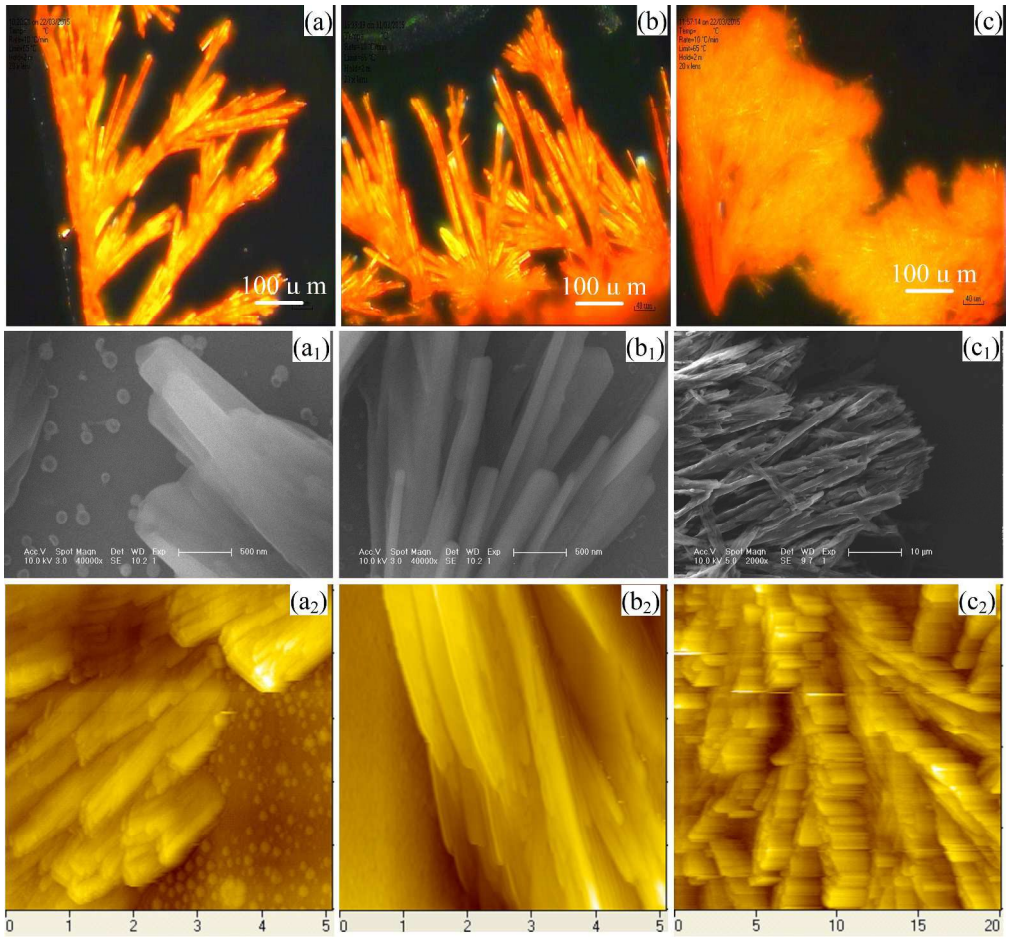

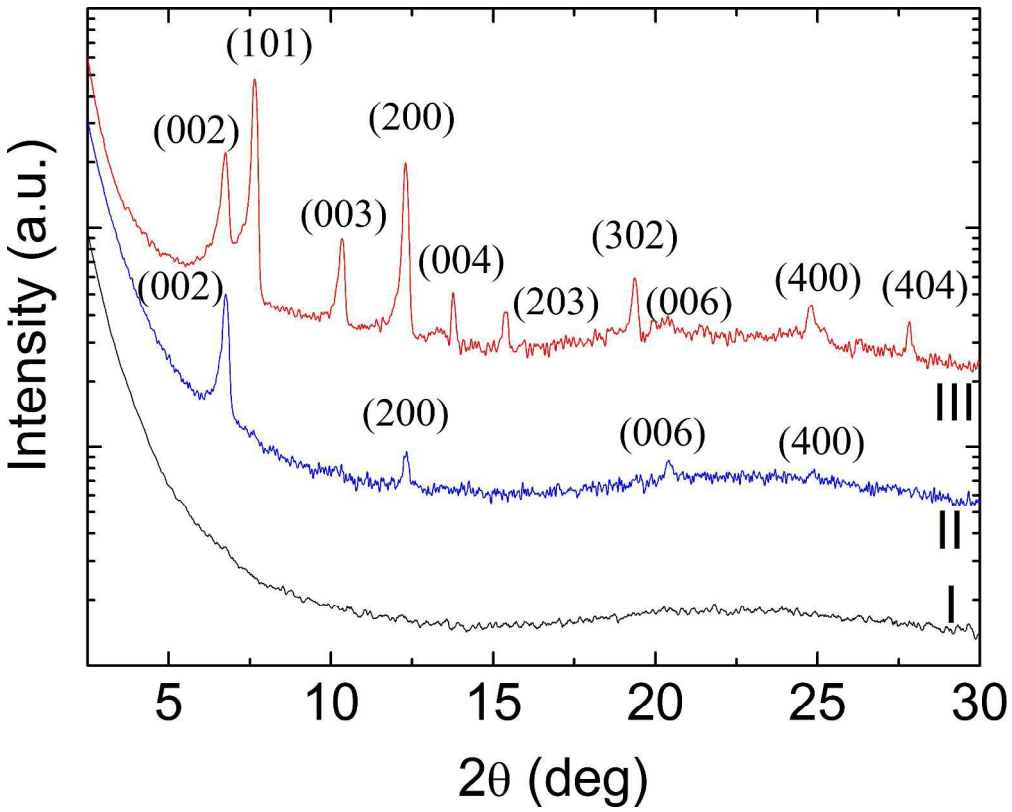

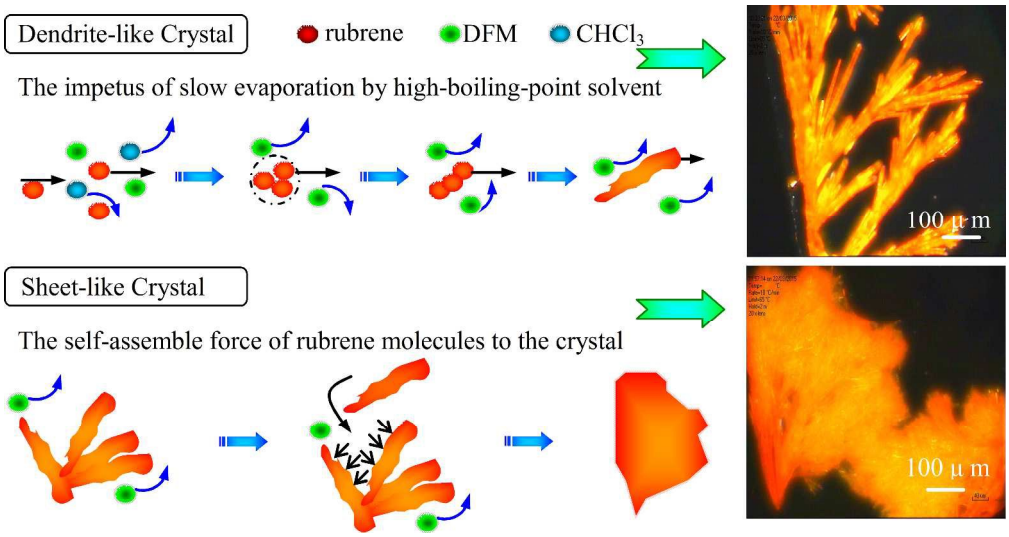

Table of Contents (ToC) graphic

Rubrene crystals have been prepared by properly tuning the blend ratio and evaporation rate of the high-boiling-point solvent.